BRIEF DEFINITIVE REPORT

Niche-specific MHC II and PD-L1 regulate CD4+CD8αα+ intraepithelial lymphocyte differentiation

Sookjin Moon[1]*, Yunji Park[2]*, Sumin Hyeon[3], Young-Min Kim[3], Ji-Hae Kim[1], Hyekang Kim[3], Subin Park[1], Kun-Joo Lee[1], Bon-Kyoung Koo[4], Sang-Jun Ha[5], and Seung-Woo Lee[1,3]

Conventional CD4+ T cells are differentiated into CD4+CD8αα+ intraepithelial lymphocytes (IELs) in the intestine; however, the roles of intestinal epithelial cells (IECs) are poorly understood. Here, we showed that IECs expressed MHC class II (MHC II) and programmed death–ligand 1 (PD-L1) induced by the microbiota and IFN-γ in the distal part of the small intestine, where CD4+ T cells were transformed into CD4+CD8αα+ IELs. Therefore, IEC-specific deletion of MHC II and PD-L1 hindered the development of CD4+CD8αα+ IELs. Intracellularly, PD-1 signals supported the acquisition of CD8αα by down-regulating the CD4-lineage transcription factor, T helper–inducing POZ/Krüppel-like factor (ThPOK), via the Src homology 2 domain–containing tyrosine phosphatase (SHP) pathway. Our results demonstrate that noncanonical antigen presentation with cosignals from IECs constitutes niche adaptation signals to develop tissue-resident CD4+CD8αα+ IELs.

Introduction

Intestinal intraepithelial lymphocytes (IELs) are a heterogeneous T cell population residing in the gut epithelium, consisting of diverse subpopulations classified by their origin and surface markers (McDonald et al., 2018). Among the subpopulations of IELs, there are phenotypically and functionally distinct subsets of CD4+ T cells that coexpress CD4 and CD8αα, CD4+CD8αα+ double-positive (DP) IELs, distinguishing them from other conventional CD4+ T helper subsets or regulatory T cells in the periphery (Cheroutre and Husain, 2013; Faria et al., 2017; Reis et al., 2013; Sujino et al., 2016). A series of reports have revealed that DP IELs originate from the conventional CD4+ T cells, including but not limited to regulatory T cells, by the transcriptional reprogramming process (Cervantes-Barragan et al., 2017; Mucida et al., 2013; Reis et al., 2013; Sujino et al., 2016). In general, conventional CD4+ and CD8+ T cells maintain their lineages by expressing T helper–inducing POZ/Krüppel-like factor (ThPOK) and runt-related transcription factor 3 (Runx3), the master transcriptional regulators of CD4 and CD8 lineages, respectively. Upon migration to the gut epithelium, the conventional CD4+ T cells lose their ThPOK, which is induced by Runx3 up-regulation, and reprogram to DP IELs in the specific gut microenvironment (Cheroutre and Husain, 2013; Mucida et al., 2013; Reis et al., 2013; Sujino et al., 2016). A subsequent study reported that T-box expressed in T cells (T-bet) is a critical upstream regulator of DP IEL differentiation, inducing Runx3 and suppressing ThPOK expression, and T-bet–inducing cytokines in the intestinal milieu such as IFN-γ preferentially promote DP IEL differentiation in the presence of gut microenvironmental cues, including TGF-β and retinoic acid (RA; Reis et al., 2014).

Studies using germ-free (GF) mice show that the gut microbiota is crucial for DP IEL development (Mucida et al., 2013; Sujino et al., 2016), and the commensal *Lactobacillus reuteri* with derivatives of dietary tryptophan was identified to promote the reprogramming of CD4+ T cells into DP IELs (Cervantes-Barragan et al., 2017). However, the detailed process that initiates TCR stimulation upon encounter of antigens, including commensal microbes, in the gut epithelium, where CD4+ T cells lose their ThPOK expression to convert to DP IELs, has not been clearly understood.

Analysis of TCR use by CD4+ single-positive (SP) and DP IELs suggests that clonal selection precedes DP IEL development

....
[1]Department of Life Sciences, Pohang University of Science and Technology, Pohang, Republic of Korea; [2]POSTECH Biotech Center, Pohang University of Science and Technology, Pohang, Republic of Korea; [3]Division of Integrative Biosciences and Biotechnology, Pohang University of Science and Technology, Pohang, Republic of Korea; [4]Institute of Molecular Biotechnology of the Austrian Academy of Sciences, Vienna Biocenter, Vienna, Austria; [5]Department of Biochemistry, College of Life Science & Biotechnology, Yonsei University, Seoul, Republic of Korea.

*S. Moon and Y. Park contributed equally to this paper; Correspondence to Seung-Woo Lee: sw_lee@postech.ac.kr; Yunji Park: yunji@postech.ac.kr.

(Cervantes-Barragan et al., 2017; Wojciech et al., 2018). This implies that MHC class II (MHC II)–mediated antigen presentation is required in the small intestine for TCR engagement of DP IELs, emphasizing the role of professional APCs expressing MHC II or other antigen presentation machinery in the intestine. However, many reports have indicated that MHC II is expressed in intestinal epithelial cells (IECs; Kambayashi and Laufer, 2014; Londei et al., 1984; Skoskiewicz et al., 1985). Furthermore, IECs regulate CD4^{+} T cells in the intestine through their MHC II (Biton et al., 2018; Koyama et al., 2019). These results led us to hypothesize that, given the unique niche for DP IELs, namely the intracellular region between IECs, MHC II antigen presentation mainly occurs in IECs for driving DP IEL differentiation.

Here, we report the evidence that IECs are key regulators that drive the differentiation of DP IELs in the intestine. We show that IECs provide TCR stimulation and coreceptor signal via their expression of MHC II and programmed death–ligand 1 (PD-L1), respectively, in a microbiota- and IFN-γ–dependent manner. Additionally, programmed cell death protein 1 (PD-1)/ PD-L1 signaling promotes down-regulation of ThPOK expression, thus turning on the lineage redirection process required for DP IEL differentiation.

Results and discussion

To address the role of IECs as atypical APCs during DP IEL differentiation, we first analyzed the expression of MHC II on IECs from the proximal to the distal part of the small intestine. We isolated IECs from the duodenum, jejunum, and ileum of naive mice and analyzed MHC II expression. Notably, MHC II expression on IECs was gradually increased from the duodenum to the ileum of the small intestine (Fig. 1 A). RNA-sequencing (RNA-seq) analysis of sorted IECs from each part of the small intestine also showed significant increases in gene expression associated with antigen processing and presentation via MHC II in the ileum (Fig. S1, A and B; and Fig. 1, B and C). Gene set enrichment analysis (GSEA) also revealed enriched expression of genes related to MHC II synthesis and antigen presentation via MHC II in the ileum compared with that in the duodenum (Fig. 1 D). Moreover, the frequency of DP IELs increased from the duodenum to the ileum (Fig. 1 E), resulting in a positive correlation between epithelial MHC II expression levels and DP IEL frequency (Fig. 1 F). This correlation was stronger at the ileum, where the abundance and diversity of microbiota are higher than in other segments (Fig. 1 F; Mowat and Agace, 2014). Interestingly, we also observed differential expression patterns of genes, including response to IFN-γ, cytokines, and the oxidation–reduction process, although the role of those genes alternatively expressed in each segment of the small intestine in DP IEL development has never been explored. The expression of *Ifngr1* and *Ifngr2* was comparable among all regions of the small intestine (Fig. S1, C–E).

To clarify the role of epithelial MHC II in the differentiation of DP IELs in vivo, we generated mice with a specific deletion of MHC II in IECs (MHC II[△IEC]; Fig. S1 G). Interestingly, we found a significant decrease of DP IEL frequencies in the small intestine

of MHC II[△IEC] compared with MHC II^{fl/fl} control (Fig. 1 G), while no significant change was detected in the other IEL subsets (Fig. S1 H). To further confirm the requirement for epithelial MHC II in DP IEL development, we analyzed immunofluorescence images of ileal tissues from MHC II^{fl/fl} and MHC II[△IEC] mice. Consistently, DP IELs were dramatically decreased in MHC II[△IEC] mice compared with those in MHC II^{fl/fl} mice (Fig. 1 H). Most DP IELs were in contact with the basolateral surface of the epithelial layer, where MHC II was highly expressed (Fig. 1 H). Thus, MHC II expression on IECs is required for the generation of DP IELs in the small intestine.

IFN-γ is a strong inducer of MHC II expression in non-hematopoietic cells, including IECs (Kambayashi and Laufer, 2014; Koyama et al., 2019; Thelemann et al., 2014). As expected, MHC II expression on IECs was not observed in IFN-γ receptor–deficient mice (IFN-γR^{−/−}; Fig. 2 A). Almost complete suppression of DP IEL development was observed in IFN-γR^{−/−} mice, and decreased expression of epithelial MHC II and frequencies of DP IELs was detected in mice receiving IFN-γ– neutralizing antibodies, indicating a causal relationship between IFN-γ–mediated MHC II expression on IECs and DP IEL differentiation (Fig. 2, A and B). Nonetheless, a previous report showed that IFN-γ is required for the differentiation of DP IELs by inducing the transcription factor T-bet, suggesting a direct role of IFN-γ in the functional maturation of DP IELs (Reis et al., 2014). Therefore, to elucidate the roles of IFN-γ in T cells or IECs for DP IEL differentiation, we generated bone marrow (BM) chimeras lacking IFN-γR expression in either nonhematopoietic or hematopoietic cells. Notably, IFN-γ directly controlled the expression of MHC II on IECs (IFN-γR^{+/+} → IFN-γR^{−/−} chimera), and the absence of IFN-γR signaling in both hematopoietic and nonhematopoietic compartments (IFN-γR^{−/−} → IFN-γR^{−/−}) prohibited DP IEL development (Fig. 2 C). However, DP IELs were dramatically decreased in mice having IFN-γR deficiency in either only hematopoietic (IFN-γR^{−/−} → IFN-γR^{+/+}) or only nonhematopoietic cells (IFN-γR^{+/+} → IFN-γR^{−/−}; Fig. 2 C). These results suggest that intact IFN-γR signaling in both hematopoietic and non-hematopoietic cells, including CD4^{+} IELs and IECs, respectively, is necessary for DP IEL differentiation. Interestingly, distinct regional differences in MHC II expression and DP IEL frequency between the proximal versus distal parts of the small intestine, as observed in the normal mice, were not detected in each BM chimeric mouse (Fig. 2 C). It is speculated that the immune reconstitution in the irradiated lymphopenic recipients may trigger the changes in gut microenvironment toward inflammatory conditions (Min, 2018), presumably by producing more IFN-γ than at the steady state, which results in the disappearance of regional differences in MHC II expression and DP IEL frequency along the small intestine.

To directly assess whether MHC II^{+} IECs acted as APCs for DP IEL differentiation, we generated the small intestine organoids and cocultured these organoids with CD4^{+} T cells. We stimulated organoids with recombinant IFN-γ for up-regulation of MHC II (Fig. 2, D and E) and pulsed them with OVA peptide (Fig. 2 F). OVA-specific CD4^{+} T cells (OT-II) were preactivated with anti-CD3ε/CD28 and then cocultured with IFN-γ–stimulated organoids in the presence of TGF-β and RA, both of which induce DP
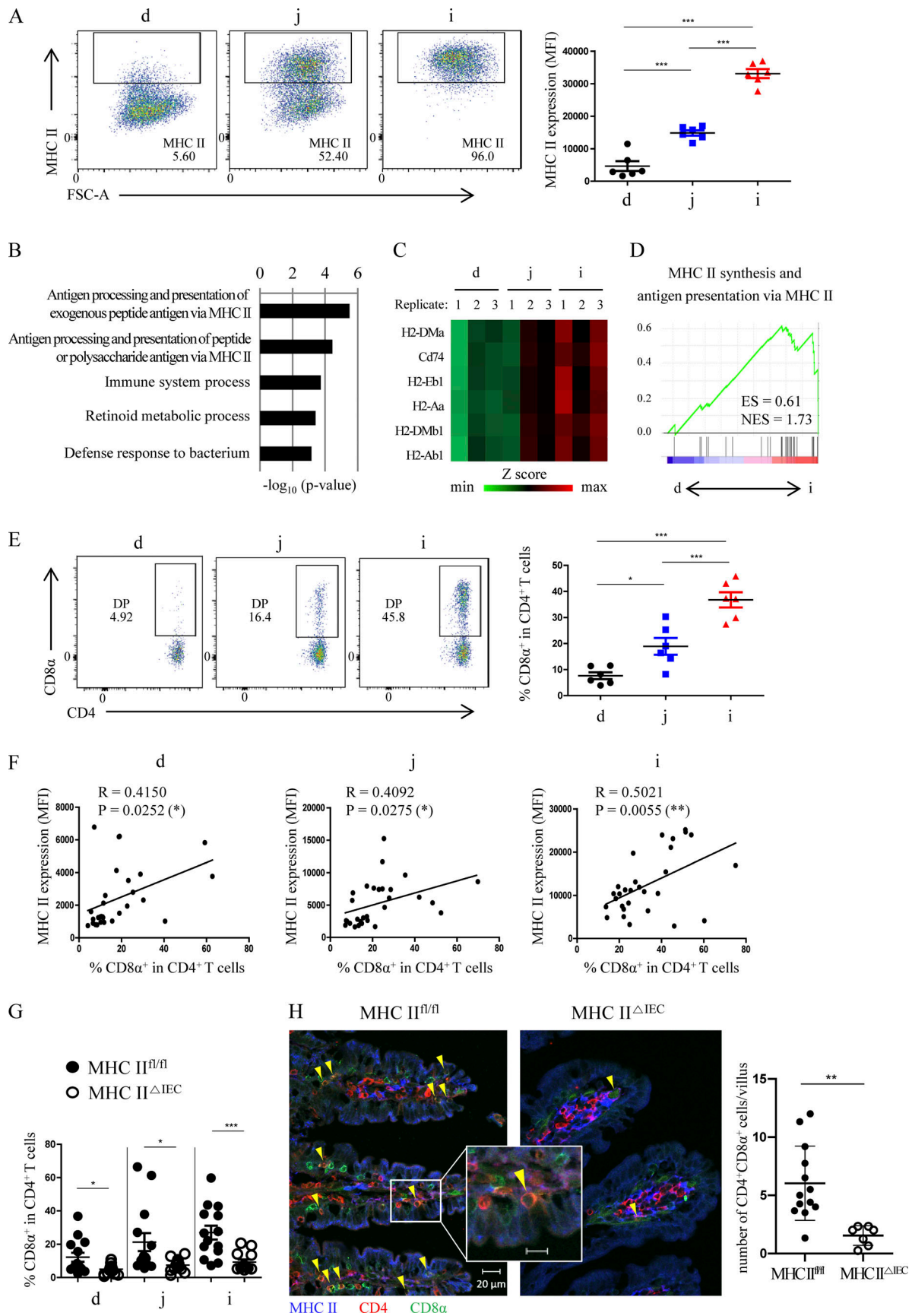
Figure 1. **MHC II expression on IECs is required for DP IEL differentiation. (A)** Representative plots (left) and MHC expression (right; mean ± SEM) on IECs (CD45.2⁻EpCAM⁺ gated) in each small intestine segment, duodenum (d), jejunum (j), and ileum (i) of C57BL/6 mice ($n = 6$). Expression level is shown as mean

fluorescence intensity (MFI). The data shown are representative of six independent experiments. **(B)** Significantly enriched GO terms of DEGs among IECs sorted from d, j, and i. **(C)** Heatmap of MHC II–related gene expression in IECs from d, j, and i of the small intestine. The same numbers under d, j, and i correspond to the replicates from the same mouse. **(D)** GSEA using gene sets of MHC class II biosynthesis (GO:0045342) and antigen processing and presentation via MHC class II (GO:0002504) for duodenal and ileal IECs. ES, enrichment score; NES, normalized enrichment score. **(E)** Representative plots (left) and DP IEL frequency (right; TCRβ⁺CD4⁺ gated; mean ± SEM) in each small intestine segment of C57BL/6 mice (n = 6). The gating strategy for DP IELs is shown in Fig. S1 F. The data shown are representative of six independent experiments. **(F)** Correlation analysis between epithelial MHC II expression and DP IEL frequency by linear regression fit in each intestinal segment (n = 29). Analysis was performed on pooled data of six independent experiments. R, correlation coefficient; P, significance of the slope. **(G)** DP IEL frequency in MHC II^fl/fl and MHC II^ΔIEC mice (n = 13–14). The data shown are pooled from five independent experiments. **(H)** Immunofluorescence images (left and middle) and quantification (right) of DP IELs in ilea of MHC II^fl/fl and MHC II^ΔIEC mice. Yellow arrowheads represent DP IELs overlapping CD4 (red) and CD8α (green). Scale bar, 20 μm or 10 μm (for inset). 7 or 13 villi from 2 mice per group were imaged and quantified. *, P < 0.05; **, P < 0.01; ***, P < 0.001. One-way ANOVA with Tukey's post hoc test (A and E) or unpaired Student's t test (G and H). FSC-A, forward scatter area.

IELs in vitro (Reis et al., 2013). TCR engagement by cognate antigen presentation through MHC II on IECs increased the differentiation of DP IELs, which was achieved with TGF-β and RA (Fig. 2 G). Collectively, these results demonstrate that IECs are atypical APCs for CD4⁺ T cells in the epithelium and that in situ differentiation of DP IELs prefers a specific anatomical location, namely the ileum of the small intestine, where IFN-γ–mediated MHC II induction prevails.

Because MHC II⁺ IECs support the cognate stimulation of CD4⁺ IELs as APCs, we hypothesized that they might express other coreceptors capable of regulating T cells in concert with MHC II. These coreceptors would be expected to be linked to IFN-γR signaling in IECs, which is critical for the MHC II expression on IECs. Therefore, we explored IFN-γ–dependent changes in gene expression in IECs by RNA-seq analysis of intestinal organoids to screen for candidate molecules that could provide cosignals to support DP IEL differentiation in the intestinal epithelium. Surprisingly, we identified *Cd274*, the gene encoding PD-L1, as the gene showing the greatest fold increase among the T cell coreceptor ligands following IFN-γ treatment in the organoids (Fig. S2, A and B). A heatmap of differentially expressed genes (DEGs) and a volcano plot revealed that *Cd274* expression was significantly increased along with MHC II–associated genes (Fig. 3, A and B). IFN-γ induced concentration-dependent up-regulation of PD-L1 protein in organoids in vitro (Fig. 3 C). The reduced epithelial PD-L1 in IFN-γR⁻/⁻ mice and in mice administered IFN-γ–neutralizing antibodies indicated the IFN-γ dependency of PD-L1 expression in IECs (Fig. 3, D and E). To further support the requirement for PD-L1 expression on IECs in DP IEL development, we analyzed DP IELs in PD-L1–silenced mice. First, PD-L1–deficient mice (PD-L1⁻/⁻) showed a significant decrease in DP IEL development, particularly in the ileum (Fig. 3 F). Second, the administration of PD-L1–neutralizing antibodies blocked DP IEL conversion when splenic CD4⁺ T cells were transferred into RAG-1–deficient mice (RAG-1⁻/⁻; Fig. 3 G). Third, we generated IEC-specific PD-L1–deficient (PD-L1^ΔIEC) mice (Fig. S3 A), and decreased DP IEL frequency was detected in the ilea of those mice (Fig. 3 H). Collectively, these results identify the important roles of PD-L1 on IECs for DP IEL development. The deficiency of PD-L1 or MHC II did not affect the expression of MHC II or PD-L1 on IECs, respectively (Fig. S3, B and C).

The microbiota was required for IFN-γ production in the intestines and for MHC II expression on IECs (Koyama et al.,

2019). Notably, DP IEL development was suppressed in GF mice (Mucida et al., 2013; Sujino et al., 2016). Thus, we next determined whether PD-L1 expression on IECs was regulated by the microbiota. Both GF and antibiotic-treated mice displayed reduced PD-L1 expression on IECs in the ileum (Fig. 4, A and B). Furthermore, epithelial MHC II expression and DP IEL development were significantly decreased in the absence of the microbiota (Fig. 4, A and B). Costaining of MHC II and PD-L1 on IECs by flow cytometry showed that most IECs expressed MHC II, and PD-L1 expression was seen only on MHC II⁺ IECs, with the fraction of MHC II⁺PD-L1⁺ cells being evidently increased in the ilea of specific pathogen–free (SPF) mice (Fig. S3 D). The immunofluorescence staining confirmed that most IECs in the ilea of SPF mice expressed MHC II, whereas ~20% of IECs displayed PD-L1 (Fig. 4 C). Consistently, greatly reduced levels of MHC II and PD-L1 were observed in the ileal epithelium of GF mice. Overall, these results suggest that microbiota-induced IFN-γ stimulates IECs to express both MHC II and PD-L1, which modulates DP IEL differentiation.

The differentiation of DP IELs requires transcriptional reprogramming of CD4⁺ T cells attributed to the loss of the CD4-lineage transcription factor, ThPOK, and acquisition of the CD8-lineage transcription factor, Runx3 (Cheroutre and Husain, 2013; Mucida et al., 2013; Reis et al., 2013). MHC II and PD-L1 on IECs play crucial roles in DP IEL differentiation, suggesting that signals elicited from the TCR and PD-1 may be involved in the reprogramming of CD4⁺ IELs. Notably, strong expression of PD-1 was observed only in induced IELs, which are developmentally derived from conventional T cells (McDonald et al., 2018), particularly CD4⁺ IELs, compared with CD8⁺ IELs (Fig. 5 A). Separation of total CD4⁺ IELs with PD-1 and CD8α positivity showed that SP IELs expressed higher levels of PD-1 than did DP IELs (Fig. 5 A). Interestingly, most SP IELs expressed PD-1, but DP IELs did not, suggesting that PD-1 expression is down-regulated during the differentiation process of SP IELs into DP IELs. The crucial role of PD-1–mediated signaling for DP IEL development was found in PD-1-deficient mice (PD-1⁻/⁻), which exhibited a greatly reduced frequency of DP IELs in the small intestine (Fig. 5 B).

To address whether PD-1 signaling regulates DP IEL differentiation in a T cell–intrinsic manner, we transferred a 1:1 mixture of splenic T cells isolated from PD-1⁺/⁺ and PD-1⁻/⁻ mice to RAG-1⁻/⁻ hosts. PD-1⁻/⁻ CD4⁺ T cells were differentiated into DP IELs less efficiently than PD-1⁺/⁺ cells in the same hosts (Fig. 5 C).
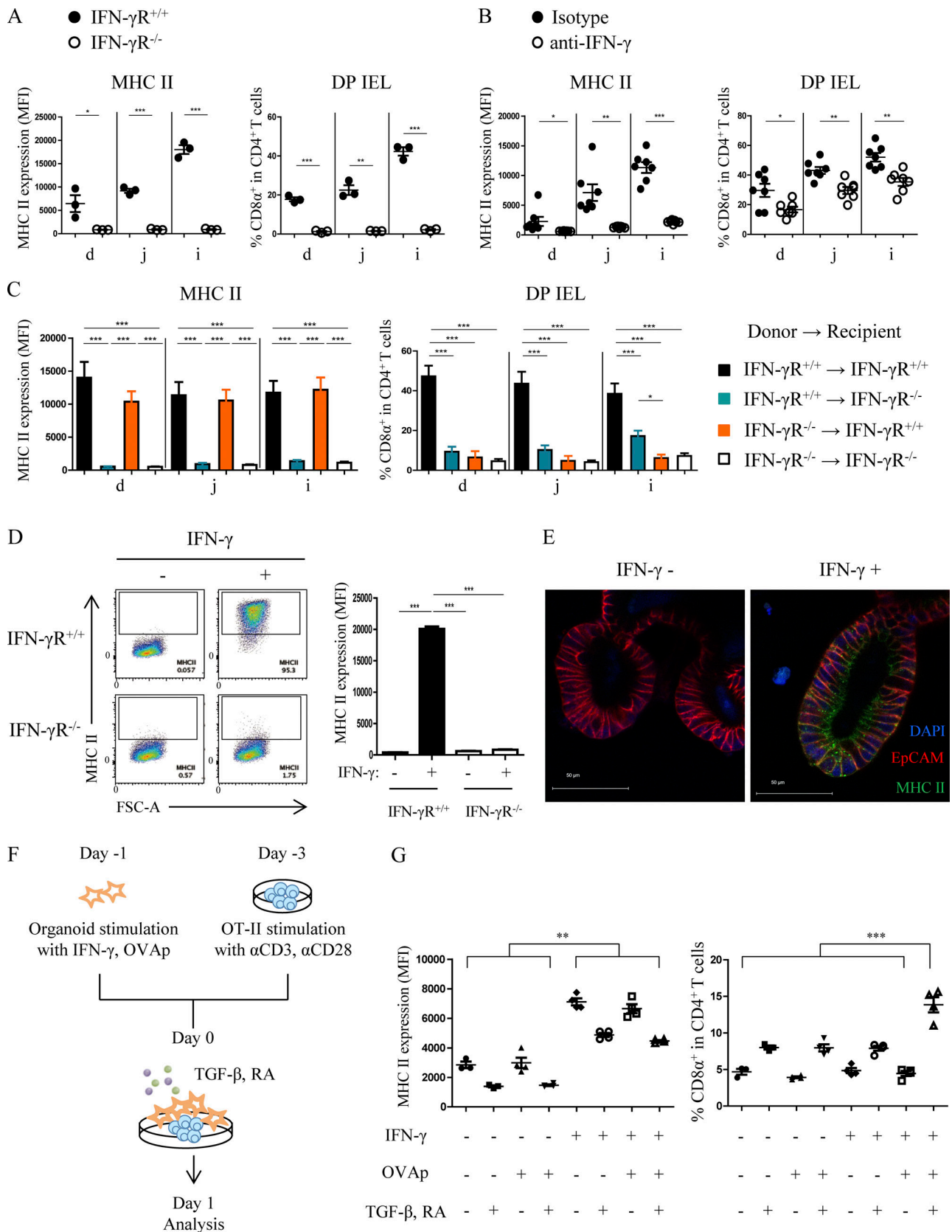
Figure 2. **MHC II expression on IECs for DP IEL differentiation is IFN-γ dependent. (A and B)** MHC II expression on IECs (left; mean ± SEM) and DP IEL frequency (right; mean ± SEM) in IFN-γR$^{+/+}$ and IFN-γR$^{-/-}$ mice (n = 3; A) and in WT mice injected with isotype or IFN-γ–neutralizing antibodies (anti–IFN-γ; n = 7; B). The data shown are representative of three (A) or two (B) independent experiments. **(C)** MHC II expression on IECs (left; mean ± SEM) and DP IEL frequency (right; mean ± SEM) in each BM chimera (n = 8–14). The data shown are pooled from two independent experiments. **(D)** Representative plots (left)

and quantification (right; mean ± SEM) of MHC II expression on organoids (gated on 7AAD⁻EpCAM⁺) derived from IFN-γR⁺/⁺ or IFN-γR⁻/⁻ mice after IFN-γ treatment for 24 h (n = 3). The data shown are representative of three independent experiments. **(E)** Immunofluorescence analysis of MHC II expression on organoids after IFN-γ treatment for 24 h. Scale bar, 50 µm. Organoids derived from C57BL/6 mice were imaged, and the data shown are representative of three independent experiments. **(F and G)** Experimental scheme of coculture system with the small intestine organoids and OT-II CD4⁺ T cells (F). MHC II expression on live IECs (GhostViolet⁻CD45⁻EpCAM⁺ gated; G, left; mean ± SEM) and live CD8α-expressing OT-II cells (GhostViolet⁻CD45⁺EpCAM⁻CD4⁺ gated; G, right; n = 3–4). The data shown are representative of two independent experiments. *, P < 0.05; **, P < 0.01; ***, P < 0.001. Unpaired Student's t test (A and B) or one-way ANOVA with Tukey's post hoc test (C, D, and G). d, duodenum; FSC-A, forward scatter area; i, ileum; j, jejunum; MFI, mean fluorescence intensity. OVAp, ovalbumin peptide.

These data suggest that T cell–intrinsic PD-1 signaling is required for DP IEL differentiation. Next, we investigated the molecular mechanisms through which PD-1 signaling modulates the transcriptional reprogramming of CD4⁺ IELs. We transferred splenic T cells from ThPOK-GFP reporter mice to RAG-1⁻/⁻ mice administered anti–PD-1 antibodies during the reconstitution period (Fig. 5 D). These results showed that loss of ThPOK and DP IEL development were inhibited by anti–PD-1 treatment (Fig. 5, E and F). Interestingly, the expression of Runx3 was unchanged by anti–PD-1 (Fig. 5 F). PD-L1–mediated downregulation of ThPOK expression was confirmed in vitro by ligation of CD4⁺ T cells with PD-L1–coated beads (Fig. 5 G). The inhibition of Src homology 2 domain–containing tyrosine phosphatase (SHP), the canonical PD-1 signaling pathway in T cells, reversed the PD-L1–induced suppression of ThPOK and CD8αα acquisition (Fig. 5, H and I). Taken together, these results suggest that PD-1 signaling through the canonical SHP pathway in CD4⁺ IELs suppresses ThPOK expression, leading to enhancement of DP IEL differentiation.

Tissue-resident T cells receive signals from tissues for their adaptation in a specific niche (Faria et al., 2017; Mueller and Mackay, 2016). Universal antigen presentation to MHC I in most nucleated cells results in CD8⁺ T cell responses to cognate antigen presented from the parenchyma of tissues, including epithelial cells (Allez et al., 2002). However, the direct antigenic stimulation of CD4⁺ T cells by epithelial cells is less likely due to the restriction of MHC II expression in professional APCs (Kambayashi and Laufer, 2014). In this study, we found that MHC II–mediated antigen presentation in IECs was required for the differentiation of CD4⁺CD8αα⁺ DP IELs. Interestingly, this epithelial MHC II–mediated regulation of CD4 IELs occurred in a specific anatomical region, namely the distal part of the small intestine. This suggests that there may be a connection with the bacterial burden of the gut microbiota, which is an essential component for MHC II expression in IECs and DP IEL development (Cervantes-Barragan et al., 2017; Koyama et al., 2019; Sujino et al., 2016). The role of TCR engagement for the development of DP IELs has recently been suggested by a study by Bilate et al., in which the researchers found that TCR signaling is required for the differentiation of SP IELs to DP IELs but not for the maintenance of DP IELs (Bilate et al., 2020). Furthermore, the inducible deletion of MHC II in IECs down-regulated the development of DP IELs. Thus, those results consistently indicate a crucial role of MHC II–mediated antigen presentation in IECs for the DP IEL differentiation. However, additional studies are required to address whether MHC II on IECs indeed presents microbiota-derived antigens or whether clones of CD4 IELs responding to microbiota antigen are differentiated into DP IELs.

Notably, we found that PD-1, a T cell coinhibitory receptor, was also involved in DP IEL differentiation. Thus, as atypical APCs, IECs induced signals in CD4⁺ T cells from the TCR and PD-1 coreceptor by up-regulating MHC II and PD-L1. PD-1 signaling blocks T cell activation signals induced by the TCR and CD28 costimulatory molecule (Hui et al., 2017; Sun et al., 2018). Interestingly, the expression of Nur77, a downstream molecule of TCR signaling, was inversely correlated with the acquisition of CD8αα, suggesting that the dampening of TCR signaling precedes DP IEL differentiation (Bilate et al., 2020). Considering that T cell–intrinsic PD-1 signaling is required for DP IEL differentiation (Fig. 5 C), we are tempted to speculate that TCR signaling is actively down-regulated by PD-1–PD-L1 interaction during DP IEL development. Undoubtedly, microbiota- and IFN-γ–dependent PD-L1 expression in IECs contributes to the ligation of PD-1 in CD4 IELs; however, the provision of PD-L1 from other cells is also possible. Therefore, during DP IEL development, clonal selection of CD4 IELs may occur via MHC II on IECs, although the differentiation of selected precursors into DP IELs may be achieved by PD-1 signaling, which down-regulates ThPOK expression via the canonical SHP pathway. We hypothesize that MHC II⁺PD-L1⁺ IECs likely regulate DP IEL differentiation as a single niche, providing TCR engagement with cognate antigen and cosignaling with PD-L1 simultaneously. However, some IELs are motile by covering a large number of IECs rather than remaining in a fixed position (Hoytema van Konijnenburg et al., 2017). Therefore, we could not rule out the possibility that CD4⁺ IELs receive alternate cues from MHC II SP IECs and then move to DP IECs.

The pivotal roles of immune–epithelium communication in the intestine have been described (Peterson and Artis, 2014). Our study indicates that the regional specification of IECs with altered gene expression contributes to their interplay with tissue-resident immune cells, adjusted to the physiological conditions in different anatomical locations. In addition to the intestines, MHC II expression has also been observed in other epithelial cells in the lungs and skin (Gereke et al., 2009; Tamoutounour et al., 2019; Wosen et al., 2018). Given the enormous surface areas of these tissues, epithelial cells may contribute to the regulation of tissue-resident CD4⁺ T cells as atypical APCs.

Materials and methods
Animal procedures
All animal experiments were performed in accordance with animal guidelines and approved by the institutional animal care and use committee of the Pohang University of Science and Technology (POSTECH; approval numbers POSTECH-2015-0065,
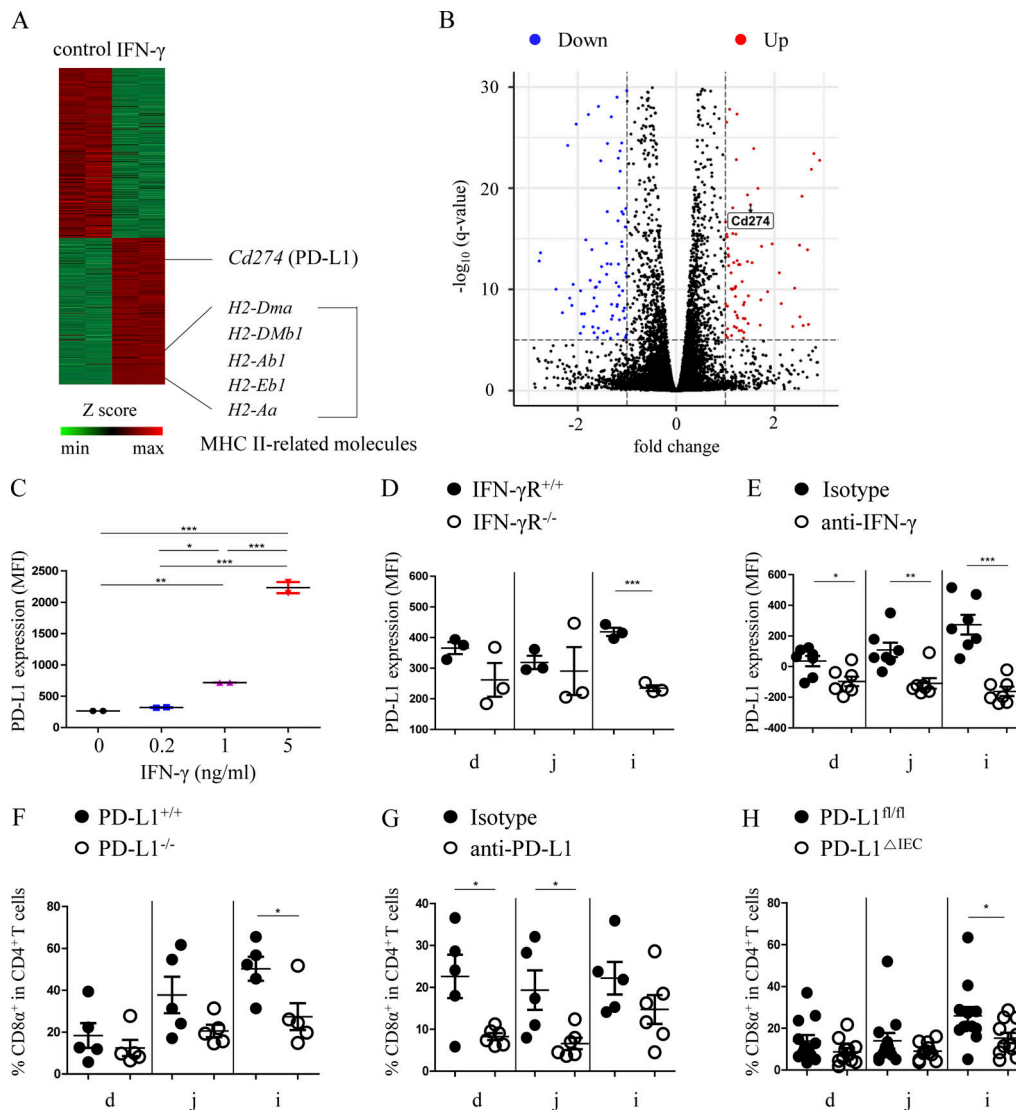
Moon et al.
MHC II and PD-L1 on IECs regulate CD4⁺CD8αα⁺ IELs

Journal of Experimental Medicine   6 of 12
https://doi.org/10.1084/jem.20201665

Figure 3. **IFN-γ–inducible PD-L1 expression on IECs is important for DP IEL differentiation. (A and B)** DEG heatmap (A) and volcano plot (B) of IFN-γ–treated and untreated (control) small intestine organoids (n = 2 per group). In the volcano plot, the x axis shows the fold change in gene expression between two groups; the y axis shows statistical significance (negative $\log_{10}$ of q value). Genes with significant fold differences after IFN-γ treatment are depicted in blue or red. **(C)** PD-L1 expression on small intestine organoids (7AAD⁻CD45⁻EpCAM⁺ gated) after IFN-γ treatment is shown as mean fluorescence intensity (MFI; n = 2). The data shown are representative of two independent experiments. **(D and E)** PD-L1 expression on IECs in IFN-γR⁺/⁺ and IFN-γR⁻/⁻ mice (n = 3; D) and on IECs in mice administered injections with isotype or anti–IFN-γ antibodies (n = 7; E). The data shown are representative of (D) or pooled from (E) two independent experiments. **(F–H)** Frequencies of DP IELs in PD-L1⁺/⁺ and PD-L1⁻/⁻ mice (n = 5; F), in splenic T cell–reconstituted RAG⁻/⁻ recipients that received injections with isotype or PD-L1–blocking antibody (anti–PD-L1) during the reconstitution period (n = 5–6; G), and in PD-L1ᶠˡ/ᶠˡ and PD-L1ᐃIEC mice (n = 12; H). The data shown are pooled from two (F) or four (H) independent experiments or are representative of two independent experiments (G). *, P < 0.05; **, P < 0.01; ***, P < 0.001. One-way ANOVA with Tukey's post hoc test (C) and unpaired Student's t test (D–H). d, duodenum; i, ileum; j, jejunum. Results (C–H) are expressed as mean ± SEM.

POSTECH-2017-0005, POSTECH-2018-0032, and POSTECH-2020-0035). All mice were on a C57BL/6 background and maintained in an SPF or GF animal facility at POSTECH. MHC IIᐃIEC mice or PD-L1ᐃIEC mice were generated by crossing H2-Ab1ᶠˡ/ᶠˡ (013181; The Jackson Laboratory) or PD-L1ᶠˡ/ᶠˡ (generated by Cyagen Co.) with Villin-cre (021504; The Jackson Laboratory) mice, respectively. Several mouse strains were generously provided: PD-L1⁻/⁻ mice by Dr. Inhak Choi, Inje University, Busan, Republic of Korea (originally generated by Dr. Lieping Chen, Yale University, New Haven, CT), IFN-γR⁻/⁻ mice

by Dr. Heung Kyu Lee (KAIST, Daejeon, Republic of Korea), PD-1⁻/⁻ mice by Dr. Sang-Nae Cho (Yonsei University, Seoul, Republic of Korea), and ThPOK-GFP mice by Dr. Daniel Mucida (The Rockefeller University, New York, NY). Mice were used at 8–16 wk of age for all experiments. Littermates or WT mice maintained by the same vivaria were used as control animals.

To generate BM chimera mice, BM cells were acquired from leg bones of donor mice by flushing with RPMI 1640 containing 5% newborn calf serum (NCS). After filtering with 40-μm mesh, 2 × 10⁶ BM cells were transferred into lethally irradiated
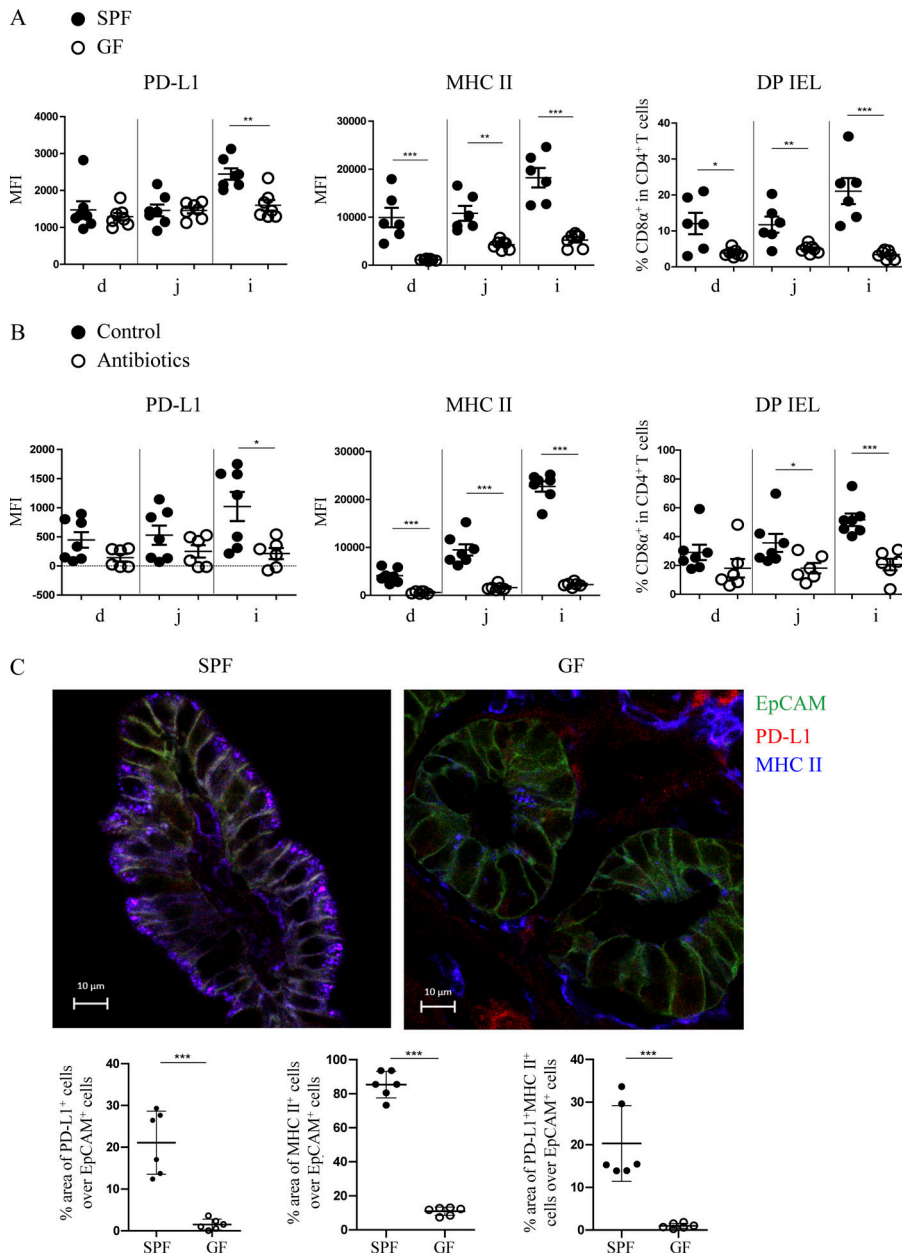
Figure 4. **The microbiota is critical for epithelial expression of MHC II and PD-L1 and DP IEL development in the small intestine. (A and B)** Epithelial expression of PD-L1 (left) and MHC II (middle) and DP IEL frequency (right) in duodenum (d), jejunum (j), and ileum (i) of GF (*n* = 6–7; A) or antibiotic-treated mice (*n* = 7; B). The data shown are pooled from two independent experiments. **(C)** Immunofluorescence images (top) and quantification (bottom) of epithelial PD-L1 and MHC II in the ilea of SPF and GF C57BL/6 mice. IECs DP for PD-L1 and MHC II are shown in purple overlapping red (PD-L1) and in blue (MHC II). The quantification data are represented as a percentage of area that stained positive for PD-L1 and MHC II over the area that stained positive for EpCAM. Scale bar, 10 µm. Six images acquired from two mice per group were quantified. *, P < 0.05; **, P < 0.01; ***, P < 0.001. Unpaired Student's *t* test (A–C). MFI, mean fluorescence intensity. Results (A–C) are expressed as mean ± SEM.

recipient mice by i.v. injection. Donor and recipient cells were distinguished with congenic markers (CD45.1, CD45.1.2, and CD45.2). After an 8 wk reconstitution period, mice were sacrificed for subsequent analysis.

For adoptive transfer experiments, T cells were purified from the spleens of ThPOK-GFP reporter mice with magnetic-activated cell sorting (Miltenyi Biotec) according to the manufacturer's protocol. 5×10^6 purified cells were transferred i.v. to RAG-1$^{-/-}$ hosts that were subsequently administered isotype control or neutralizing antibodies against PD-1 or PD-L1 (anti–PD-1, BE0273; isotype for anti–PD-1, BE0089; anti–PD-L1, BE0101; isotype for anti–PD-L1, BE0090; all from Bio X Cell) i.p. for 4 wk (100 µg twice per week). For IFN-γ blockade, mice were administered i.p. injections with control or IFN-γ–neutralizing antibodies (anti–IFN-γ, BE0054; isotype for anti–IFN-γ, BE0088; all from Bio X Cell) for 2 wk (100 µg twice per week).

To deplete the gut microbiota, an antibiotic cocktail consisting of 0.5 g/liter of vancomycin, 1.0 g/liter of ampicillin, 1.0 g/liter of neomycin, and 1 g/liter of metronidazole, which were all purchased from Sigma-Aldrich (vancomycin, V1130; ampicillin, A0166; neomycin, N6386; metronidazole, M1547), was administered to SPF C57BL/6 mice in drinking water for 4 wk.

Antibodies and flow cytometry
Single-cell suspensions were preincubated with antimouse CD16/32 for 15 min on ice before surface marker staining to block Fc receptors and then subsequently stained with the following fluorophore-conjugated antibodies according to the manufacturer's recommended concentrations for 15 min on ice. Antibodies were purchased from eBioscience (anti-CD4, 48-0042-82; anti-CD8α, 25-0081-82; anti-CD45.2, 11-0454-81; anti–PD-L1, 46-5982-82; anti–MHC class II, 48-5321-82 or 47-
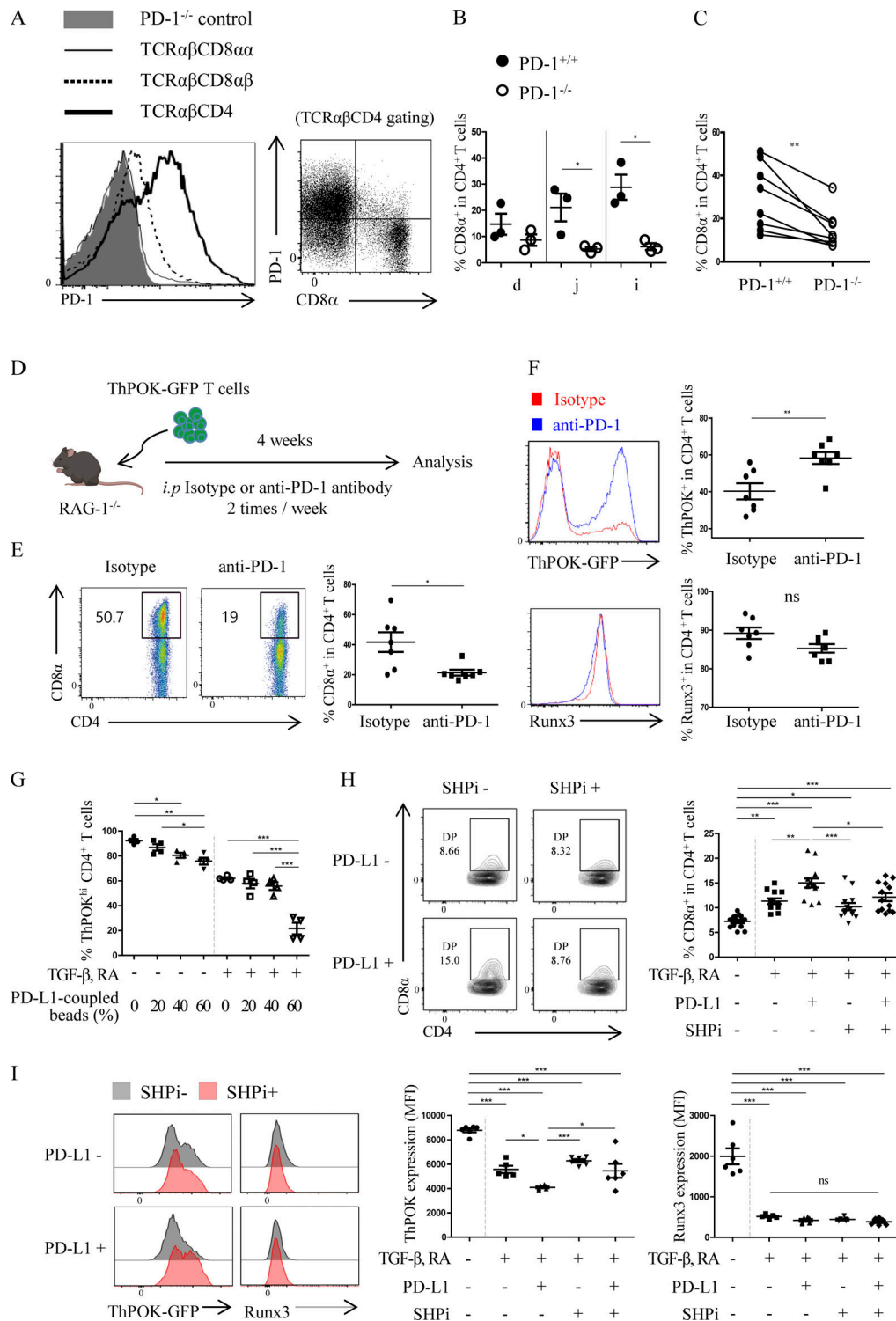
Figure 5. **PD-1 signaling–mediated ThPOK suppression induces DP IEL generation. (A)** PD-1 expression on each IEL subset (left) and separation of TCRαβ⁺CD4⁺ IELs depending on the expression of PD-1 and CD8α (right) in C57BL/6 mice. **(B)** The frequency of DP IELs in PD-1⁺/⁺ and PD-1⁻/⁻ mice (n = 3; mean ± SEM). The data shown are representative of two independent experiments. **(C)** Generation of DP IELs in RAG⁻/⁻ recipients transferred with a 1:1 mixture of PD-1⁺/⁺ and PD-1⁻/⁻ splenic T cells. The frequency of DP IELs in PD-1⁺/⁺ and PD-1⁻/⁻ T cell donors from the same recipient are connected by a line (n = 8). The data shown are representative of three independent experiments. **(D–F)** Experimental scheme (D), representative plots (left) and frequency (right; mean ± SEM) of DP IELs (E), and expression of ThPOK or Runx3 (F; mean ± SEM) in RAG⁻/⁻ recipients administered injections with isotype or PD-1 receptor–blocking antibody (anti–PD-1) during the reconstitution period (all gated on TCRβ⁺CD4⁺ T cells; n = 7). The data shown are pooled from two independent experiments. **(G)** The frequency of ThPOKhi cells (mean ± SEM) after 3 d in in vitro culture of CD4⁺ T cells in the presence of TGF-β, RA, and epoxy beads covalently coated with different amounts of PD-L1 protein. The percentage of PD-L1–coated beads represents the amount of PD-L1 protein over total protein coated on beads (n = 4). The data shown are pooled from two independent experiments. **(H and I)** Representative plots (H and I; left) and quantification of CD8α induction (H; right; mean ± SEM) and

ThPOK (I; middle; mean ± SEM) or Runx3 (I; right) expression in CD4⁺ T cells cultured for 3 d in the presence of TGF-β, RA, plate-coated PD-L1, and SHP inhibitor (SHPi; n = 5–13). The data shown are pooled from two or four independent experiments. *, P < 0.05; **, P < 0.01; ***, P < 0.001; ns, not significant. Unpaired (B, E, and F) or paired (C) Student's t test and one-way ANOVA with Tukey's post hoc test (G–I). d, duodenum; i, ileum; j, jejunum.

5321-82; anti-TCRβ, 45-5961-82; anti-ThPOK, 12-5928-80), Bio-Legend (anti-CD16/32, 101302; anti-CD8β, 126605; anti–PD-L1, 124308; anti–PD-1, 135210 or 135227; anti-CD326, 118212; anti-TCRγ/δ, 118108; anti–granzyme B, 372221), and R&D Systems (anti-Runx3, IC3765A). For live/dead staining, Ghost Dye Violet 510 viability dye (13-0870-T100; Tonbo Biosciences) or 7-aminoactinomycin D (7-AAD, 51-68981E; BD Biosciences) was used. For intracellular staining, a Foxp3/transcription factor fixation/permeabilization kit was used (00-5521-00; eBioscience). Data were acquired with an LSR Fortessa 5 laser analyzer or BD FACSCanto II analyzer (both from BD Biosciences) and analyzed with FlowJo software (FlowJo, LLC).

Isolation of IECs and IELs
IECs and IELs of the small intestines were isolated with some modifications to the protocol described previously (Mucida et al., 2007). Briefly, the small intestines were isolated and placed in chilled RPMI 1640 media containing 5% NCS. After removal of fat tissues and Peyer's patches, the intestines were opened longitudinally and cut into the duodenum, jejunum, and ileum. The intestinal tissue was transferred to a 50-ml Falcon tube containing 20 ml of RPMI 1640 supplemented with 5% NCS and 2 mM EDTA. After the samples were shaken at 250 rpm for 40 min at 37°C, the tissue suspension was pelleted by centrifugation at 1,500 rpm for 10 min at 4°C. The cell pellet was resuspended, layered to a 40%/70% Percoll gradient, and centrifuged at 2,500 rpm for 30 min. Enriched cells, which contained IECs and IELs, were collected and washed for the subsequent staining process.

In vitro CD4⁺ T cell cultures
CD4⁺ T cells were purified from splenocytes by magnetic-activated cell sorting according to the manufacturer's protocol. Purified cells were cultured for 3 d in 96-well plates precoated with 5 μg/ml of anti-CD3ε and 2.5 μg/ml of soluble anti-CD28 (anti-CD3ε, 40-0031-M001; anti-CD28, 40-0281-U500; Tonbo Biosciences). For induction of CD4⁺CD8αα⁺ cells, CD4⁺ T cells were stimulated with 10 nM RA (R2625; Sigma-Aldrich) and 2 ng/ml TGF-β (100-21; PeproTech) during the culture period. For ligating T cells with PD-L1–conjugated beads, CD4⁺ T cells were stimulated with Dynabeads (14011; Thermo Fisher Scientific) coated with anti-CD3ε, anti-CD28, and Fc control (BE0096; Bio X Cell) or recombinant mouse PD-L1-Fc (provided by Genexine Co.) according to the manufacturer's protocol. Briefly, 10⁷ beads were coated with anti-CD3ε (1 μg; 20% of total protein), anti-CD28 (1 μg; 20% of total protein), Fc control (3 μg, 2 μg, 1 μg, or 0 μg; 60%, 40%, 20%, or 0% of total protein, respectively), and PD-L1-Fc (0 μg, 1 μg, 2 μg, or 3 μg; 0%, 20%, 40%, or 60% of total protein, respectively, coated according to the amount of Fc control to make a final 100% of protein coating for beads). For some T cell cultures, 10 μM SHP1/2 protein-tyrosine phosphatase inhibitor (565851; Merck) was added to 96-well plates precoated with PD-L1-Fc.

Generation of intestinal organoids and coculture with CD4⁺ T cells
Intestinal organoids were prepared as previously described (Sato et al., 2009). Briefly, the mouse small intestine was opened longitudinally, and the contents were removed by washing with cold PBS. The intestine was incubated with PBS supplemented with 2 mM EDTA for 1 h at 4°C to isolate crypts. Isolated crypts were filtered through a 70-μm cell strainer and were centrifuged at 4°C and 900 g for 5 min. Approximately 500 crypts were mixed with 20 μl of Matrigel (356231; BD Biosciences) and plated in 48-well plates. After polymerization of Matrigel, we added 300 μl of culture media (12634-010; Invitrogen) containing penicillin-streptomycin (15140-122), GlutaMAX (35050-061), Hepes (15630-080; all from Gibco), N-2 supplement (17502-048), B-27 supplement (17504-044; all from Invitrogen), N-acetyl-L-cysteine (A9165; Sigma-Aldrich), epidermal growth factor (315-09-1000), R-spondin 1 (120-38-1200), and Noggin (250-38-100; all from PeproTech). Fresh media were replaced every 2–3 d, and organoids were passaged every week with a 1:3 split ratio. For coculture with T cells, organoids were stimulated in the presence of 5 ng/ml of IFN-γ (315-05; PeproTech) and 30 μg/ml of OVA₃₂₃₋₃₃₉ peptide (synthesized by Peptron) for 24 h. CD4⁺ T cells isolated from OT-II mice were stimulated for 3 d in 96-well plates coated with anti-CD3ε and soluble anti-CD28. 10⁵ stimulated CD4⁺ T cells and roughly 50–100 organoids were seeded together into round-bottom 96-well plates, with 10 nM of RA and 2 ng/ml of TGF-β. Cells were analyzed after 24 h of coculture.

Immunofluorescence staining and image quantification
Freshly isolated mouse ileal tissues were opened and washed with clean PBS three times. Tissues were fixed in 4% paraformaldehyde at 4°C overnight and were washed with clean PBS. Samples were frozen in optimum cutting temperature compound (Tissue-Tek). 10–20-μm cryosections were acquired from the optimum cutting temperature compound block of ileal tissues by using a Leica CM1850 cryostat. Each section was incubated with a blocking solution of 1% BSA with 0.5% Triton X-100 in PBS for 2 h at RT. After being washed with PBS, antibodies (diluted 1:100) were added to the section and incubated at 4°C overnight. After being washed with PBS, samples were mounted and imaged. Antibodies were purchased from eBioscience (anti-CD4, 12-0042-82; anti–MHC II, 17-5321-82 or 48-5321-82), BD Pharmingen (anti-CD8α; 557668), Invitrogen (anti–PD-L1; 12-5982-82), and BioLegend (antimouse epithelial cell adhesion molecule [EpCAM]; 118212). The cell nucleus was stained with a mountant with DAPI purchased from Invitrogen (P36931). Images were acquired using an LSM 700 confocal microscope, Axio Observer (Zeiss).

Automated quantification was performed using ImageJ software provided by the National Institutes of Health. For the quantification of epithelial expression of MHC II and PD-L1, the area that stained positive for MHC II and PD-L1 was measured over the area that stained positive for EpCAM, and the percentage of area occupancy was calculated. To quantify the number of DP IELs, circularly shaped cells that stained positive for both CD4 and CD8α were automatically counted per villus.

RNA-seq analysis

Total RNA was extracted from FACS-sorted epithelial cells (CD45⁻EpCAM⁺) from the small intestines or intestinal organoids. cDNA was synthesized with a QuantiTect Reverse Transcription Kit (205311; QIAGEN). The library for RNA-seq analysis was generated using the TruSeq RNA Sample Prep Kit version 2 or the TruSeq Stranded Total RNA LT Sample Prep Gold Kit and sequenced on a HiSeq 4000 system. For the analysis of IECs, expression data were normalized as a $\log_2$-transformed fragments per kilobase of transcript per million mapped reads value. DEGs were defined as genes of mouse replicate number 1 with fold change ≥3 between duodenum and ileum and fold change ≥1.5 between duodenum and jejunum. Visualization of enriched Gene Ontology (GO) terms in DEGs was performed as previously described (Bonnot et al., 2019). For the analysis of epithelial cells from organoids, raw sequencing data were quantified with kallisto (mm10 was used for the mouse reference genome), and the R library sleuth and EnhancedVolcano were used for data processing and plotting. To draw a DEG heatmap, expression data were normalized as $\log_2$-transformed (transcripts per million +1) values, and genes with fold changes greater than or equal to one between the average of nontreated and IFN-γ–treated organoids were used. DAVID (version 6.7) and the GO resource were used for GO analysis. GSEA was performed using GSEA software (version 4.0) provided by the Broad Institute.

Statistics

Statistical analysis was performed using GraphPad Prism software, and the tests used are indicated in the figure legends.

Data availability

The RNA-seq data of IECs sorted from three segments of the small intestine and untreated or IFN-γ–treated intestinal organoids have been deposited in the ArrayExpress archive and are available under accession numbers E-MTAB-9744 and E-MTAB-9756, respectively.

Online supplemental material

Fig. S1 relates to Fig. 1 and shows RNA-seq analysis of IECs sorted from each small intestine section, the gating scheme for DP IELs, and epithelial MHC II expression or IEL subsets in MHC II△IEC mice. Fig. S2 relates to Fig. 3 and shows enriched GO terms of DEGs or fold increases in gene expression of T cell coreceptor ligands between untreated and IFN-γ–treated organoids. Fig. S3 relates to Fig. 3 and shows the expression of PD-L1 and/or MHC II on IECs in C57BL/6, PD-L1△IEC, MHC II△IEC, or GF mice.

References

Allez, M., J. Brimnes, I. Dotan, and L. Mayer. 2002. Expansion of CD8⁺ T cells with regulatory function after interaction with intestinal epithelial cells. *Gastroenterology.* 123:1516–1526. https://doi.org/10.1053/gast.2002.36588

Bilate, A.M., M. London, T.B.R. Castro, L. Mesin, J. Bortolatto, S. Kongthong, A. Harnagel, G.D. Victora, and D. Mucida. 2020. T cell receptor is required for differentiation, but not maintenance, of intestinal CD4⁺ intraepithelial lymphocytes. *Immunity.* 53:1001–1014.e20. https://doi.org/10.1016/j.immuni.2020.09.003

Biton, M., A.L. Haber, N. Rogel, G. Burgin, S. Beyaz, A. Schnell, O. Ashenberg, C.W. Su, C. Smillie, K. Shekhar, et al. 2018. T helper cell cytokines modulate intestinal stem cell renewal and differentiation. *Cell.* 175:1307–1320.e22. https://doi.org/10.1016/j.cell.2018.10.008

Bonnot, T., M.B. Gillard, and D.H. Nagel. 2019. A simple protocol for informative visualization of enriched Gene Ontology terms. *Bio-101.* e3429.

Cervantes-Barragan, L., J.N. Chai, M.D. Tianero, B. Di Luccia, P.P. Ahern, J. Merriman, V.S. Cortez, M.G. Caparon, M.S. Donia, S. Gilfillan, et al. 2017. *Lactobacillus reuteri* induces gut intraepithelial CD4⁺CD8αα⁺ T cells. *Science.* 357:806–810. https://doi.org/10.1126/science.aah5825

Cheroutre, H., and M.M. Husain. 2013. CD4 CTL: living up to the challenge. *Semin. Immunol.* 25:273–281. https://doi.org/10.1016/j.smim.2013.10.022

Faria, A.M.C., B.S. Reis, and D. Mucida. 2017. Tissue adaptation: Implications for gut immunity and tolerance. *J. Exp. Med.* 214:1211–1226. https://doi.org/10.1084/jem.20162014

Gereke, M., S. Jung, J. Buer, and D. Bruder. 2009. Alveolar type II epithelial cells present antigen to CD4⁺ T cells and induce Foxp3⁺ regulatory T cells. *Am. J. Respir. Crit. Care Med.* 179:344–355. https://doi.org/10.1164/rccm.200804-592OC

Hoytema van Konijnenburg, D.P., B.S. Reis, V.A. Pedicord, J. Farache, G.D. Victora, and D. Mucida. 2017. Intestinal epithelial and intraepithelial T cell crosstalk mediates a dynamic response to infection. *Cell.* 171:783–794.e13. https://doi.org/10.1016/j.cell.2017.08.046

Hui, E., J. Cheung, J. Zhu, X. Su, M.J. Taylor, H.A. Wallweber, D.K. Sasmal, J. Huang, J.M. Kim, I. Mellman, et al. 2017. T cell costimulatory receptor CD28 is a primary target for PD-1-mediated inhibition. *Science.* 355:1428–1433. https://doi.org/10.1126/science.aaf1292

Kambayashi, T., and T.M. Laufer. 2014. Atypical MHC class II-expressing antigen-presenting cells: can anything replace a dendritic cell? *Nat. Rev. Immunol.* 14:719–730. https://doi.org/10.1038/nri3754

Koyama, M., P. Mukhopadhyay, I.S. Schuster, A.S. Henden, J. Hülsdünker, A. Varelias, M. Vetizou, R.D. Kuns, R.J. Robb, P. Zhang, et al. 2019. MHC class II antigen presentation by the intestinal epithelium initiates graft-versus-host disease and is influenced by the microbiota. *Immunity.* 51: 885–898.e7. https://doi.org/10.1016/j.immuni.2019.08.011

Londei, M., J.R. Lamb, G.F. Bottazzo, and M. Feldmann. 1984. Epithelial cells expressing aberrant MHC class II determinants can present antigen to cloned human T cells. *Nature.* 312:639–641. https://doi.org/10.1038/312639a0

McDonald, B.D., B. Jabri, and A. Bendelac. 2018. Diverse developmental pathways of intestinal intraepithelial lymphocytes. *Nat. Rev. Immunol.* 18:514–525. https://doi.org/10.1038/s41577-018-0013-7

Min, B. 2018. Spontaneous T cell proliferation: a physiologic process to create and maintain homeostatic balance and diversity of the immune system. *Front. Immunol.* 9:547. https://doi.org/10.3389/fimmu.2018.00547

Mowat, A.M., and W.W. Agace. 2014. Regional specialization within the intestinal immune system. *Nat. Rev. Immunol.* 14:667–685. https://doi.org/10.1038/nri3738

Mucida, D., Y. Park, G. Kim, O. Turovskaya, I. Scott, M. Kronenberg, and H. Cheroutre. 2007. Reciprocal T_H17 and regulatory T cell differentiation mediated by retinoic acid. *Science.* 317:256–260. https://doi.org/10.1126/science.1145697

Mucida, D., M.M. Husain, S. Muroi, F. van Wijk, R. Shinnakasu, Y. Naoe, B.S. Reis, Y. Huang, F. Lambolez, M. Docherty, et al. 2013. Transcriptional reprogramming of mature CD4+ helper T cells generates distinct MHC class II–restricted cytotoxic T lymphocytes. *Nat. Immunol.* 14:281–289. https://doi.org/10.1038/ni.2523

Mueller, S.N., and L.K. Mackay. 2016. Tissue-resident memory T cells: local specialists in immune defence. *Nat. Rev. Immunol.* 16:79–89. https://doi.org/10.1038/nri.2015.3

Peterson, L.W., and D. Artis. 2014. Intestinal epithelial cells: regulators of barrier function and immune homeostasis. *Nat. Rev. Immunol.* 14: 141–153. https://doi.org/10.1038/nri3608

Reis, B.S., A. Rogoz, F.A. Costa-Pinto, I. Taniuchi, and D. Mucida. 2013. Mutual expression of the transcription factors Runx3 and ThPOK regulates intestinal CD4+ T cell immunity. *Nat. Immunol.* 14:271–280. https://doi.org/10.1038/ni.2518

Reis, B.S., D.P. Hoytema van Konijnenburg, S.I. Grivennikov, and D. Mucida. 2014. Transcription factor T-bet regulates intraepithelial lymphocyte functional maturation. *Immunity.* 41:244–256. https://doi.org/10.1016/j.immuni.2014.06.017

Sato, T., R.G. Vries, H.J. Snippert, M. van de Wetering, N. Barker, D.E. Stange, J.H. van Es, A. Abo, P. Kujala, P.J. Peters, et al. 2009. Single Lgr5 stem cells build crypt-villus structures in vitro without a mesenchymal niche. *Nature.* 459:262–265. https://doi.org/10.1038/nature07935

Skoskiewicz, M.J., R.B. Colvin, E.E. Schneeberger, and P.S. Russell. 1985. Widespread and selective induction of major histocompatibility complex-determined antigens in vivo by gamma interferon. *J. Exp. Med.* 162:1645–1664. https://doi.org/10.1084/jem.162.5.1645

Sujino, T., M. London, D.P. Hoytema van Konijnenburg, T. Rendon, T. Buch, H.M. Silva, J.J. Lafaille, B.S. Reis, and D. Mucida. 2016. Tissue adaptation of regulatory and intraepithelial CD4+ T cells controls gut inflammation. *Science.* 352:1581–1586. https://doi.org/10.1126/science.aaf3892

Sun, C., R. Mezzadra, and T.N. Schumacher. 2018. Regulation and function of the PD-L1 checkpoint. *Immunity.* 48:434–452. https://doi.org/10.1016/j.immuni.2018.03.014

Tamoutounour, S., S.J. Han, J. Deckers, M.G. Constantinides, C. Hurabielle, O.J. Harrison, N. Bouladoux, J.L. Linehan, V.M. Link, I. Vujkovic-Cvijin, et al. 2019. Keratinocyte-intrinsic MHCII expression controls microbiota-induced Th1 cell responses. *Proc. Natl. Acad. Sci. USA.* 116: 23643–23652. https://doi.org/10.1073/pnas.1912432116

Thelemann, C., R.O. Eren, M. Coutaz, J. Brasseit, H. Bouzourene, M. Rosa, A. Duval, C. Lavanchy, V. Mack, C. Mueller, et al. 2014. Interferon-γ induces expression of MHC class II on intestinal epithelial cells and protects mice from colitis. *PLoS One.* 9:e86844. https://doi.org/10.1371/journal.pone.0086844

Wojciech, L., E. Szurek, M. Kuczma, A. Cebula, W.R. Elhefnawy, M. Pietrzak, G. Rempala, and L. Ignatowicz. 2018. Non-canonicaly recruited TCRαβCD8αα IELs recognize microbial antigens. *Sci. Rep.* 8:10848. https://doi.org/10.1038/s41598-018-29073-7

Wosen, J.E., D. Mukhopadhyay, C. Macaubas, and E.D. Mellins. 2018. Epithelial MHC class II expression and its role in antigen presentation in the gastrointestinal and respiratory tracts. *Front. Immunol.* 9:2144. https://doi.org/10.3389/fimmu.2018.02144
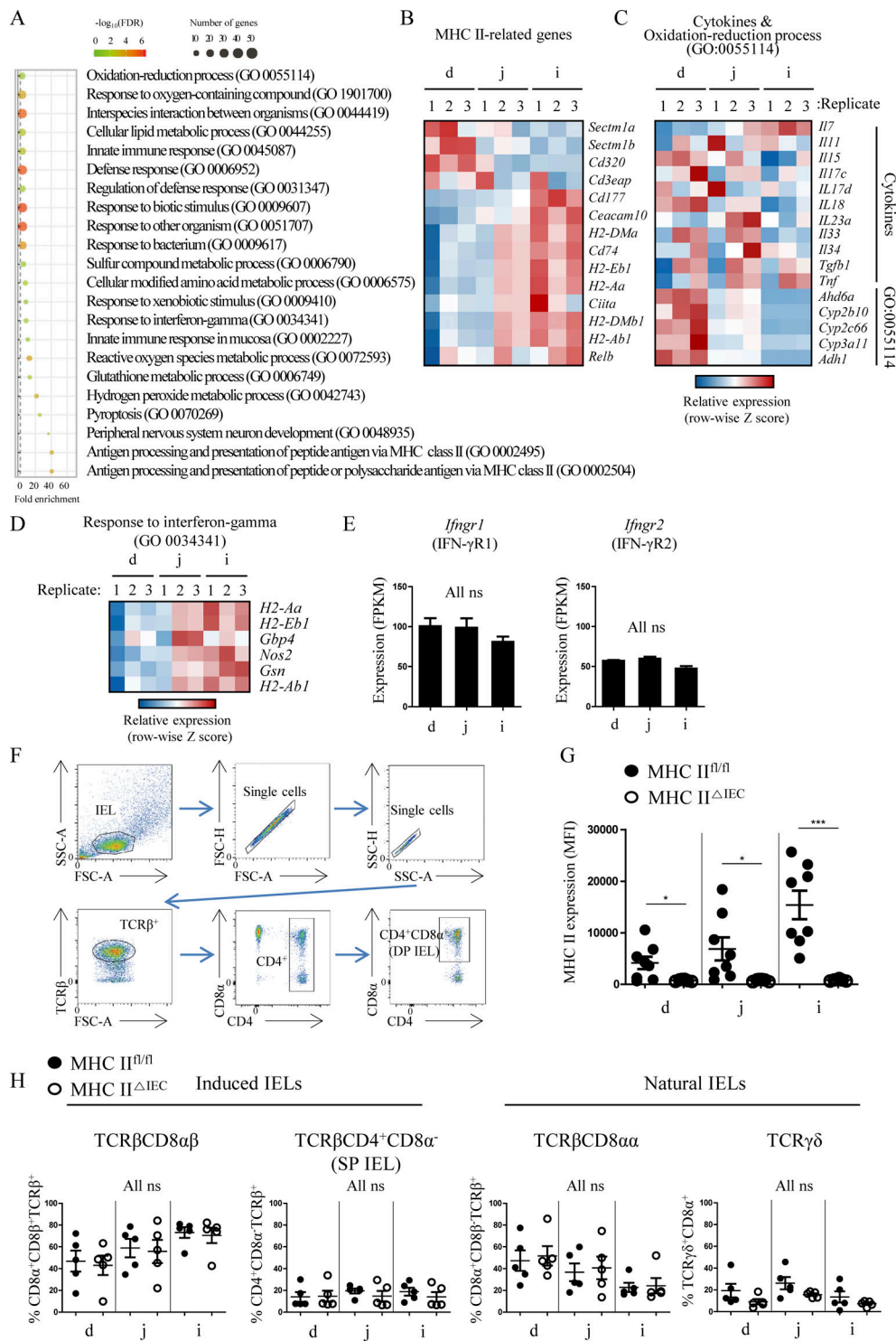
Figure S1. **MHC II expression on IECs is enriched in the distal small intestine, constituting a favorable niche for differentiation of DP IELs but not other IEL subtypes. (A)** Significantly enriched GO terms of DEGs among IECs sorted from duodenum (d), jejunum (j), and ileum (i). DEG analysis was performed using the PANTHER classification system. **(B–D)** Heatmap of MHC II–related genes (B), cytokines and DEGs annotated in oxidation–reduction process (GO: 0055114; C), and DEGs annotated in response to IFN-γ (GO:0034341; D). The same numbers below d, j, and i correspond to the replicates from the same mouse. **(E)** Expression of *Ifngr1* and *Ifngr2* from RNA-seq analysis of IECs sorted from d, j, and i (mean ± SEM). **(F)** Gating scheme of DP IELs. **(G)** MHC II expression (mean fluorescence intensity [MFI]; mean ± SEM) on IECs in d, j, and i of MHC II$^{fl/fl}$ and MHC II$^{\Delta IEC}$ mice (n = 8). The data shown are pooled from three independent experiments. **(H)** Frequencies of IEL subsets in MHC II$^{fl/fl}$ and MHC II$^{\Delta IEC}$ mice (n = 5; mean ± SEM). The data shown are pooled from two independent experiments. IEL populations were gated as TCRβ⁺CD4⁻CD8α⁺CD8β⁺ (TCRβCD8αβ), TCRβ⁺CD4⁺CD8α⁻ (TCRβCD4⁺CD8α⁻; SP IEL), TCRβ⁺CD4⁻CD8α⁺CD8β⁻ (TCRβCD8αα), or TCRγδ⁺CD8α⁺ (TCRγδ). *, $P < 0.05$; ***, $P < 0.001$, ns, not significant. One-way ANOVA with Tukey's post hoc test (E) or unpaired Student's t test (G and H). FDR, false discovery rate; FSC-A, forward scatter area; FSC-H, forward scatter height; SSC-A, side scatter area; SSC-H, side scatter height.
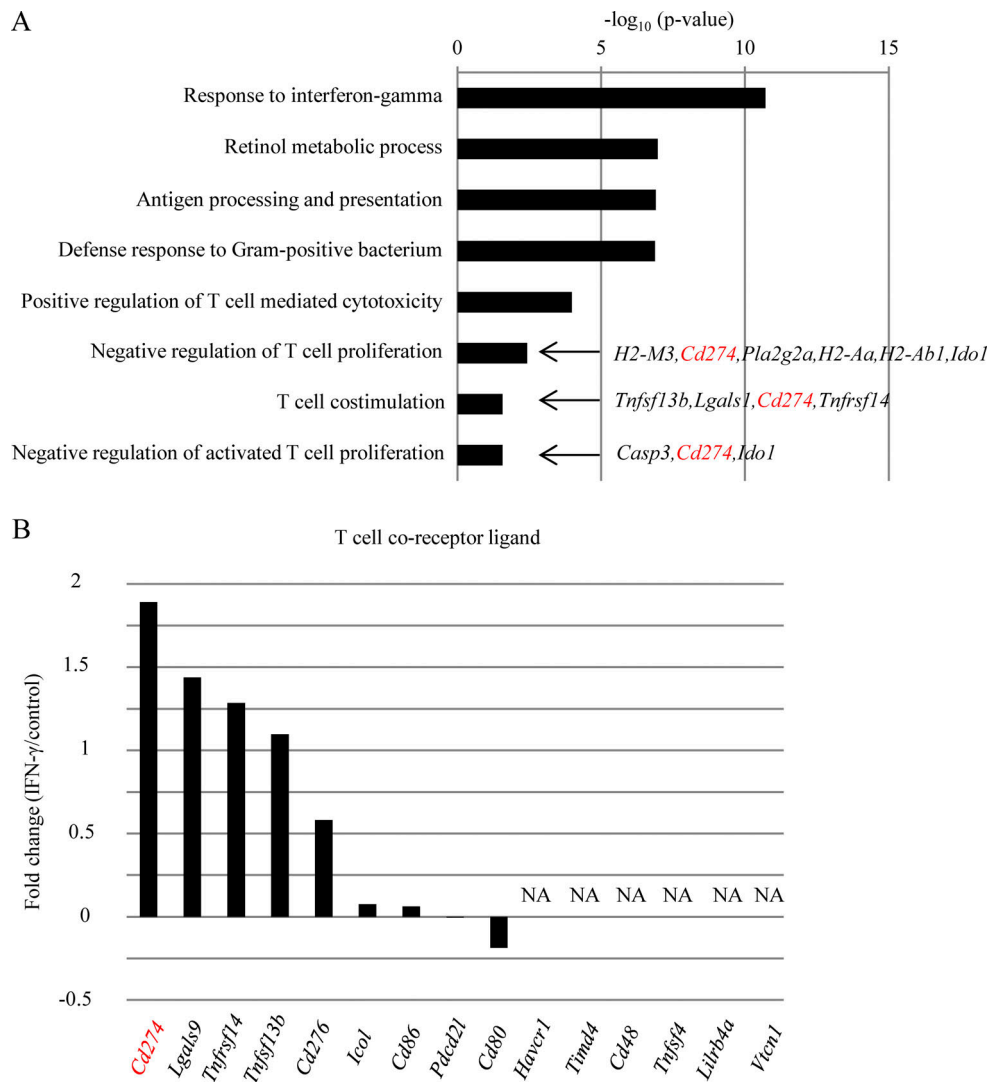
A

-log₁₀ (p-value)

Response to interferon-gamma
Retinol metabolic process
Antigen processing and presentation
Defense response to Gram-positive bacterium
Positive regulation of T cell mediated cytotoxicity
Negative regulation of T cell proliferation ← *H2-M3,Cd274,Pla2g2a,H2-Aa,H2-Ab1,Ido1*
T cell costimulation ← *Tnfsf13b,Lgals1,Cd274,Tnfrsf14*
Negative regulation of activated T cell proliferation ← *Casp3,Cd274,Ido1*

B

T cell co-receptor ligand

Fold change (IFN-γ/control)

NA NA NA NA NA NA

Cd274 Lgals9 Tnfrsf14 Tnfsf13b Cd276 Icol Cd86 Pdcd21 Cd80 Havcr1 Timd4 Cd48 Tnfsf4 Lilrb4a Vtcn1

Figure S2. **Increase of *Cd274* expression in the IFN-γ–treated intestinal organoids. (A)** Enriched GO terms of DEGs between untreated and IFN-γ–treated organoids. **(B)** Fold change in gene expression of T cell coreceptor ligands in IFN-γ–treated over untreated organoids. NA, not applicable.
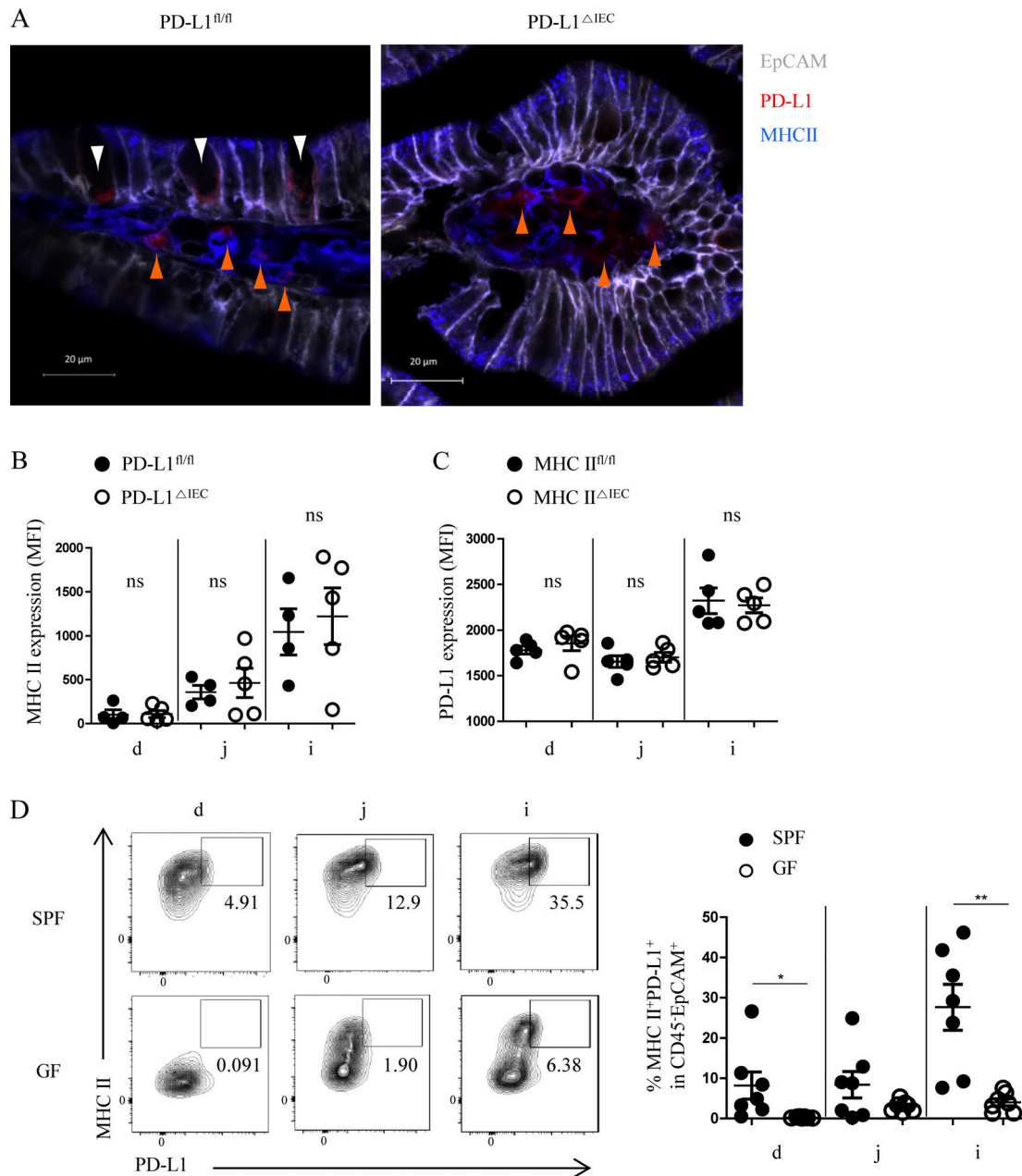
Figure S3. **Expression of both PD-L1 and MHC II on IECs is regulated by environmental factors including the microbiota rather than by each other's expression. (A)** Immunofluorescence analysis showing PD-L1 and MHC II expression on IECs in the ileal villi of PD-L1$^{fl/fl}$ or PD-L1$^{\triangle IEC}$ mice. Scale bar, 20 µm. Two mice per group were imaged, and the data shown are representative of two independent experiments. IECs and lamina propria cells positive for PD-L1 are indicated by white and orange arrowheads, respectively. **(B and C)** MHC II expression and PD-L1 expression (mean ± SEM) on IECs in PD-L1$^{\triangle IEC}$ (B) and MHC II$^{\triangle IEC}$ (C) mice, respectively (n = 4–5). The data shown are pooled from two independent experiments. **(D)** Representative plots (left) and frequencies (right; mean ± SEM) of IECs expressing both MHC II and PD-L1 (CD45$^-$EpCAM$^+$ gated) in each small intestine segment (n = 7). The data shown are pooled from two independent experiments. *, P < 0.05; **, P < 0.01; ns, not significant. Unpaired Student's t test (B–D). d, duodenum; i, ileum; j, jejunum.